Geoderma 442 (2024) 116773

Contents lists available at ScienceDirect

Geoderma

journal homepage: www.elsevier.com/locate/geoderma

Advancing noninvasive and nondestructive root phenotyping techniques: A two-phase permittivity model for accurate estimation of root volume

Huijie Gu [a,b], Imre Cseresnyés [c], John R. Butnor [d], Baoru Li [a,b], Hongyong Sun [a], Xiying Zhang [a], Yang Lu [a], Xiuwei Liu [a,b,*]

[a] Key Lab of Agricultural Water Resources, the Innovative Academy of Seed Design, The Center for Agricultural Resources Research, Institute of Genetics and Developmental Biology, The Chinese Academy of Sciences, 286 Huaizhong Road, Shijiazhuang, Hebei 050022, China
[b] University of Chinese Academy of Sciences, 19 Yuquan Road, Beijing 100049, China
[c] Institute for Soil Sciences, HUN-REN Centre for Agricultural Research, H-1022 Budapest, Herman Ottóút 15., Hungary
[d] USDA Forest Service, Northern Research Station, 81 Carrigan Drive, Aiken Center, Room 208C, University of Vermont, Burlington, VT 05405, USA

ARTICLE INFO

Handling Editor: Y. Capowiez

Keywords:
Soil electrical capacitance
Root volume
High frequency
Theoretical model
Nondestructively

ABSTRACT

Noninvasive and nondestructive root phenotyping techniques under field conditions are needed to advance plant root science. Soil electrical parameters including capacitance and resistance hold potential to meet this need, although their specific ability to detect roots remains uncertain. In this study, we developed a two-phase root and soil permittivity model at high frequency enabling accurate and noninvasive prediction of root volume. The validation calculation showed that the two-phase model successfully predicts root volume with a minimal error of less than 1 % under the control conditions with roots placed in wet soil and water. Furthermore, we demonstrated that the high-frequency bulk soil capacitance when integrated into an empirical model, can accurately estimate root volume for summer maize (*Zea mays* L.) in both the field (root mean square error (RMSE) = 1.52 cm^3) and in root washing-free measurement applications in the absence of soil (RMSE = 0.36 cm^3). When the empirical relationship between high-frequency bulk soil capacitance and root volume is not adequate, the two-phase model can be used to calibrate the empirical model. To this end, a series of soil pot experiments with winter wheat (*Triticum aestivum* L.) showed that the measurement accuracy can be fundamentally improved. These results highlighted the effectiveness of the two-phase permittivity model, making high-frequency bulk soil capacitance a reliable method for *in situ* measurement of root volume. It is anticipated that the availability of new equipment for measuring high-frequency soil electrical parameters will lead to widespread adoption of this root phenotyping technique in the future.

1. Introduction

Roots play a vital role in plants, serving as their anchor and facilitating crucial functions such as nutrient and water uptake. Additionally, they contribute to soil carbon and nitrogen cycling through root exudates and fine root turnover. Improving the utilization efficiency of water and fertilizer is important for increasing crop production and can be augmented by selecting genotypes with desirable root traits for given environment (Lynch, 2013; Lynch, 2019; Karlova et al., 2021). However, the lack of in-situ nondestructive, noninvasive, and high-throughput crop root phenotyping methods hinders the optimization of root functionality.

Electrical methods such as electrical capacitance (EC), electrical resistance (ER), electrical impedance tomography, electrical resistivity tomography and spectral induced polarization approaches, offer noninvasive, nondestructive, and rapid deployment for high-throughput applications (Mancuso, 2012; Cimpoiasu et al., 2020; Ehosioke et al., 2020). EC, for instance, can be categorized into stem-based

Abbreviations: EC, Electrical capacitance; EC_{system}, electrical capacitance for stem, root and medium; EC_{medium}, medium electrical capacitance; EC_{soil}, Soil electrical capacitance without roots; EC_{root}, Root electrical capacitance; EC_{S+R}, Soil electrical capacitance with roots; EC_{water}, Water electrical capacitance without roots; EC_{W+R}, Water electrical capacitance with roots; SWC, Soil water content.

* Corresponding author at: Key Lab of Agricultural Water Resources, the Innovative Academy of Seed Design, The Center for Agricultural Resources Research, Institute of Genetics and Developmental Biology, The Chinese Academy of Sciences, 286 Huaizhong Road, Shijiazhuang, Hebei 050022, China (X. Liu).
E-mail address: xwliu@sjziam.ac.cn (X. Liu).

https://doi.org/10.1016/j.geoderma.2024.116773
Received 18 August 2023; Received in revised form 22 December 2023; Accepted 3 January 2024
Available online 13 January 2024
0016-7061/© 2024 The Authors. Published by Elsevier B.V. This is an open access article under the CC BY license (http://creativecommons.org/licenses/by/4.0/).

measurement (including stem, root and medium EC (EC_{system}), where one electrode is inserted on the stem and the other one in the medium) and medium-based measurement (medium capacitance (EC_{medium}), with both electrodes located in the medium) (Tsukanov and Schwartz, 2021). Although EC_{system} predicts root properties such as root surface area, root dry mass and root volume by measuring the EC_{system} between stem and substrate (Chloupek, 1972; Dalton, 1995; Ehosioke et al., 2020; Ellis et al., 2013a,b), concerns have been raised about the ability of EC_{system} to accurately quantify root size, as electrical current can escape from the root surface (Peruzzo et al., 2020). Gu et al. (2021) recently found that alternating current (AC) can flow through the roots under dry soil conditions, and hence, EC_{system} can estimate root traits under dry soil conditions rather than under wet conditions. When the medium containing roots is subjected to low frequency (<1 kHz) AC, the presence of an electrical double layer leads to counterion polarization of root cells, which allows the root system to have a large permittivity, increasing the permittivity of the medium (Weigand and Kemna, 2017, 2019; Tsukanov and Schwartz, 2021), as a result, root characteristics may be sensed by EC_{medium} with root (EC_{M+R}) (Liao et al., 2015; Mary et al., 2017; Tsukanov and Schwartz, 2020). Indeed, bulk medium such as soil polarization is composed of root polarization and soil colloid polarization (Kessouri et al., 2019), the volume fraction of crop roots in the bulk soil is generally low (for example, around 0.006 for wheat, 0.02 for maize, and 0.006 for rice in top 10 cm soil layer) meaning the contribution of the root system to the polarization of the medium tends to be minimal at low frequency (Gan et al., 2011). Since plant root growth and uptake affect soil water status, ion content and porosity, they also induce changes in soil polarization (Tsukanov and Schwartz, 2023). Consequently, the polarization of the medium at low frequency may serve as an indicator of root uptake.

However, to date, EC_{system} has been unable to effectively estimate root traits based on the empirical model particularly because the signal from roots is lost to background noise from the soil. The measurements are difficult to interpret without a theoretical model. Indeed, the dispersion ranges of α, β, and γ overlap to some extent for biological materials. Generally, the α-dispersion covers frequencies from a few Hz up to 10 kHz. The β-dispersion spans from a few kHz to 100 MHz, and the γ-dispersion extends from 100 MHz to 100 GHz. The polarization mechanism transfers from counterion polarization (<20 kHz) to interfacial (kHz–MHz, high-frequency in this paper), orientation (MHz–GHz), ion (approximately 10^{12} Hz), and electron (10^{12}–10^{15} Hz) polarization as the frequency increases. As stated before, low-frequency EC_{M+R} does not measure crop root traits directly. In contrast, using high-frequency EC_{M+R} to measure roots seems promising recently. As known, the root cell (μm) is much smaller than the soil aggregate particle (mm), and the root cell is surrounded by cell walls and epidermis, which are not contained around the soil particles. Thus, roots are much more quickly charged than soil at high frequencies, which is evidenced by the higher electrical conductivity and permittivity of roots than soil (Rajkai et al., 2005; Weigand and Kemna, 2019; Basak and Wahid, 2022). This means that roots contribute more to the high-frequency bulk soil polarization than soil, which supports our speculation that high-frequency EC_{M+R} may be used to indicate root information. Basak and Wahid (2022) may be the first to report that medium impedance magnitude at high frequency (5 kHz–100 kHz) is negatively correlated with root size (weight and length) of carrots via a root burying experiment. The close correlation is further confirmed by our previous observations conducted in soil pots and field experiments (Gu et al., 2023). Because the relationships between root traits and impedance magnitude/capacitance are caused by root addition, these relationships are causal. However, it is important to highlight that the mechanism and applicability of using high-frequency EC_{M+R} to measure roots remain unexplored. To fully explore the potential of this approach, the objectives of the present study are to (1) develop a theoretical model for root detection and a practical means of deploying it under different conditions and (2) investigate the potential mechanism of using high-frequency EC_{M+R} to measure roots.

2. Model development

The mechanism of high-frequency medium polarization can be described by the classical Maxwell-Wagner's Eq (1). (Maxwell, 1891; Wagner, 1914):

$$\varepsilon^* = \varepsilon_m^* \frac{2\varepsilon_m^* + \varepsilon_i^* - 2\Phi(\varepsilon_m^* - \varepsilon_i^*)}{2\varepsilon_m^* + \varepsilon_i^* + \Phi(\varepsilon_m^* - \varepsilon_i^*)} = \varepsilon_m^*(1 + 3\Phi \frac{(\varepsilon_m^* - \varepsilon_i^*)}{2\varepsilon_m^* + \varepsilon_i^* + \Phi(\varepsilon_m^* - \varepsilon_i^*)}) \tag{1}$$

where ε^* is the complex relative permittivity of the non-uniform system, ε_m^* is the complex relative permittivity of the medium, ε_i^* is the complex relative permittivity of the dielectric sphere in the medium, Φ is the volume fraction of the dielectric sphere. Assuming that the Φ is far less than 1 (Maxwell, 1891), ($\Phi \pm 1$) multiplied by any parameter (γ) can be simplified to γ ($\Phi \pm 1) \approx \gamma$. The complex relative permittivity of the continuous system can be expressed in Eq. (2):

$$\varepsilon^* \approx \varepsilon_m^*(1 + 3\Phi \frac{\varepsilon_i^* - \varepsilon_m^*}{2\varepsilon_m^* + \varepsilon_i^*}) \tag{2}$$

Eq. (2) explains the linear negative correlation between root systems size and electrical impedance at high frequency reported in Basak and Wahid (2022) because electrical impedance and complex permittivity are negatively correlated (Eq. (3)).

$$Z = \frac{d}{sk^*} = \frac{d}{js\omega\varepsilon_0\varepsilon^*}, \tag{3}$$

where Z represents electrical impedance, k^* is the complex conductivity, ω (=2πf) is angular frequency, j is an imaginary unit, ε_0 is the vacuum permittivity, and s and d represent the area and distance of the electrode plate, respectively.

However, Li et al. (2020) demonstrated that although the real part of electrical impedance does not perform well in detecting roots, the imaginary part proves to be effective. The electrical impedance is the reciprocal of the complex conductance. The relationship between the complex conductivity and the complex permittivity shows that the imaginary part of the complex conductivity corresponds to the real part of the complex permittivity (Eq. (4)).

$$k^* = k + jk'' = \omega\varepsilon_0\varepsilon'' + j\omega\varepsilon_0\varepsilon = j\omega\varepsilon_0\varepsilon^* \tag{4}$$

where k is the real part of the complex conductivity, k'' is the imaginary part of the complex conductivity, ε is the real part of the complex permittivity, ε'' is the imaginary part of the complex permittivity.

The polarization of a substance can be described by the real part of its complex relative permittivity (corresponding to the imaginary part of electrical impedance) and shows potential for root size detection as discussed before. Substituting Eq. (5) into Eq. (1) derives the separation Eq. (6)) of the real part of Eq. (1) (Debye, 1912, Zhao, 2008).

$$\varepsilon^* = \varepsilon - j\left(\frac{k}{\omega\varepsilon_0}\right), \tag{5}$$

$$\varepsilon(\omega) = \varepsilon_\infty + \frac{\Delta\varepsilon}{1 + (\omega\tau)^2}, \tag{6}$$

where

$$\varepsilon_\infty = \varepsilon_m \frac{2\varepsilon_m + \varepsilon_i - 2\Phi(\varepsilon_m - \varepsilon_i)}{2\varepsilon_m + \varepsilon_i + \Phi(\varepsilon_m - \varepsilon_i)} \approx \varepsilon_m\left(1 + 3\Phi\frac{\varepsilon_i - \varepsilon_m}{2\varepsilon_m + \varepsilon_i}\right), \tag{7}$$

$$\Delta\varepsilon = \frac{9\Phi(1-\Phi)(\varepsilon_m k_i - \varepsilon_i k_m)^2}{[2\varepsilon_m + \varepsilon_i + \Phi(\varepsilon_m - \varepsilon_i)][2k_m + k_i + \Phi(k_m - k_i)]^2} \approx \frac{9\Phi(\varepsilon_m k_i - \varepsilon_i k_m)^2}{(2\varepsilon_m + \varepsilon_i)(2k_m + k_i)^2}, \tag{8}$$

$$\tau = \varepsilon_0 \frac{2\varepsilon_m + \varepsilon_i + \Phi(\varepsilon_m - \varepsilon_i)}{2k_m + k_i + \Phi(k_m - k_i)} \approx \varepsilon_0 \frac{2\varepsilon_m + \varepsilon_i}{2k_m + k_i}, \tag{9}$$

where ε_∞ is the limit of permittivity at high frequency, $\Delta\varepsilon$ is dielectric increment, τ is relaxation time. k_m and k_i are the conductivity of the medium and dielectric sphere, respectively.

In order to simplify the Eqs. (7)–(9), three coefficients were proposed:

$$a = \varepsilon_m k_i - \varepsilon_i k_m \tag{10}$$

$$b = 2\varepsilon_m + \varepsilon_i \tag{11}$$

$$c = 2k_m + k_i \tag{12}$$

A new Eq. (13) is derived by combining Eqs. (5)–(12):

$$\varepsilon(\omega) = \Phi\left(\frac{9a^2}{\omega^2 b^3 \varepsilon_0^2 + bc^2} + 3\varepsilon_m \frac{\varepsilon_i - \varepsilon_m}{b}\right) + \varepsilon_m \tag{13}$$

To simplify Eq. (13), there are two basic preconditions for replacing the dielectric sphere with the root system in the complex relative permittivity of the medium: (1) The permittivity of root system is greater than that of medium without roots, such that EC_{root} greatly contributes to EC_{M+R}; (2) the product of the permittivity of roots and electrical conductivity of the medium without roots is much greater than the product of the permittivity of medium without roots and electrical conductivity of roots, such that the interface polarization can be induced. At β (kHz-MHz) dispersion, the relative permittivity of biological materials (around 10^4–10^5 in the frequency of 10 kHz–100 kHz) is much greater than that of the medium (<100 in the frequency of 10 kHz–100 kHz) (Kuang and Nelson, 1998, Mancuso, 2012, Zajicova and Chuman, 2019). We performed a data pre-analysis and found that the relative permittivity of roots was 200 and 300 times greater than that of soil and water under frequency of 30 kHz–60 kHz, respectively, and the values of root relative permittivity multiplied by medium electrical conductivity were also much greater than those of medium relative permittivity multiplied by root conductivity (more than 59 and 73 times for soil and water under frequency of 30 kHz–60 kHz, respectively, see the Results section). Thus, the coefficients of a and b can be further simplified as $a \approx -\varepsilon_i k_m$ and $b \approx \varepsilon_i$. Therefore, the correlation between permittivity and volume fraction of live root growth medium at β dispersion can be approximated by Eq. (14):

$$\varepsilon(\omega) \approx \Phi\left[\frac{9\varepsilon_i k_m^2}{(2k_m + k_i)^2 + \omega^2 \varepsilon_0^2 \varepsilon_i^2} + 3\varepsilon_m\right] + \varepsilon_m \tag{14}$$

When the frequency is lower than 100 kHz, the cellular entry for current is impeded; conversely, when the frequency is higher than 100 kHz, the current permeates through the cell membrane (Mancuso, 2012; Ehosioke et al., 2020). Therefore, root system morphology affects the measurement outcomes. The shape of the root system can be approximately treated as a cylindrical non-sphere. For the same permittivity increase, the volume required for the sphere is 3/2 times of that of the cylinder (Zhao, 2008). Therefore, Eq. (14) can be rewritten as follows:

$$\varepsilon(\omega) \approx \frac{3}{2}\Phi\left[\frac{9\varepsilon_i k_m^2}{(2k_m + k_i)^2 + \omega^2 \varepsilon_0^2 \varepsilon_i^2} + 3\varepsilon_m\right] + \varepsilon_m \tag{15}$$

However, the cells that make up the root system can be regarded as spheres, so further study is required to examine whether Eq. (14) or Eq. (15) is more suitable for calculating root volume.

3. Materials and methods

Four experiments were conducted in this study (Table 1 and Supplementary Fig. 1). The first experiment involved root additions to water or soil, referred to as root immersing/burying experiments. This experiment was designed to develop and verify the two-phase model. The second experiment involved collecting soil samples containing roots from the field and measuring root volume without washing out the

Table 1
The experimental summary.

Experiments		Plant species	Medium	Treatments	Frequency	SWC during measurement (g/g)	Purpose
Experiment 1	Test 1	Wheat	Water Soil		20–500 kHz (500)	Saturated	To verify the rationality of the simplified formula and the validity of the calculation of root volume
	Test 2	Wheat	Water				
	Test 3	Wheat	Soil			Saturated	
	Root immersing	Maize	Water	Same root size	20–500 kHz (500)		To explore the effect of roots on the medium EC under different conditions
	Root burying	Maize	Top soil			Saturated	
	Root burying	Maize	Sand			0.1, 0.2, 0.25	
			Top soil			0.05, 0.1, 0.2, 0.25	
	Root immersing	Wheat	Water		20–501 kHz (51)		
	Root immersing	Wheat	Water	Different root size	50–100 kHz (10)		To explore the relationship between medium EC and root volume
	Root burying	Wheat	Top soil			Saturated	
Experiment 2	Soil core sampling	Maize	Soil		20–500 kHz (500)	Saturated	To explore the feasibility of replacing root cleaning based on EC_{S+R}
Experiment 3	Pot 1	Wheat	Top soil	Dry/deficit	50–100 kHz (10)	Saturated	To apply different models for root volume estimation
	Pot 2	Wheat	Top soil	Wet/dry	50–100 kHz (10)	Saturated	To explore the effects of root absorption function and root polarization on EC_{S+R}
Experiment 4	Field	Maize	Soil		20–500 kHz (500)	0.15–0.23	To test whether EC_{S+R} can measure the root depth distribution in the field

Note: the number in parentheses indicates the number of measured frequencies. SWC indicates soil water content. EC indicates electrical capacitance. EC_{S+R} indicates electrical capacitance of soil with roots. $EC_{water:}$ electrical capacitance of water.

roots, known as the root washing-free experiment. This experiment was used to test the application of the two-phase model. The third experiment was a soil pot experiment, the fourth one was a field experiment, and both aimed at *in situ* root measurements (Table 1). Field topsoil (0–20 cm) was collected at Luancheng Agro-Eco-Experimental Station of the Chinese Academy of Sciences (37°53′N, 114°41′E, altitude: 50.1 m) located in Shijiazhuang, China and then sieved through a 2.5 mm sieve to remove large plant litter for root burying and soil pot experiments. The soil texture was identified as silty loam (Haplic luvisol according to FAO-WRB; IUSS Working Group, 2015) and other detailed physico-chemical properties can be found in Gu et al. (2021). The root samples for the root immersing and root burying experiments were obtained from the wheat and maize field at Luancheng Agro-Eco-Experimental Station. The EC and ER of all experiments were measured at an output voltage of 1 V in parallel mode.

3.1. Experiment 1: Root immersing/burying experiments

3.1.1. Root immersing and burying experiments for the two-phase model development

To determine whether the derivation process of the two-phase model is reasonable and whether Eq. (14) or (15) can be used as a theoretical model to directly calculate root volume, a series of root immersing and burying experiments were conducted.

Three tests of EC_{root} and ER_{root} measurements were conducted to calculate the root volume using the two-phase model. In the first test (Test 1), EC_{medium} and ER_{medium} were measured on a soil with a fixed volume (188.16 cm^3), and EC_{root} and ER_{root} were measured separately for each root. Second, EC_{medium} and ER_{medium} were measured on water, but EC_{root} and ER_{root} were measured for several random root samples (Test 2). Third, EC_{medium} and ER_{medium} were measured on a sampling soil from a large amount of sieved soil. Similarly, EC_{root} and ER_{root} were measured for a few samples from a large set of fresh samples (Test 3). For the Test 1, 20 wheat roots with a length of 6 cm and a relatively uniform diameter at heading stage were selected. Before adding roots to the medium, the soil was fully saturated, and EC_{soil} and ER_{soil} were measured. Next, the LCR-meter test clips were used to clamp both the ends of a single root to measure EC_{root} and ER_{root} and the root length and dimeter were determined later. Then these 20 roots were buried into the wet soil and EC_{S+R} and ER_{S+R} were measured again. Test 1 was also repeated in a water medium. For Test 2, EC_{water} and ER_{water} were measured before adding roots, and EC_{W+R} was measured after adding roots. Then 24 roots were randomly selected from a large set of fresh root samples to measure EC_{root} and ER_{root} in the same way as the Test 1. The length and diameter of each root were then measured. Subsequently, four different amounts roots were added into the water and EC_{W+R} and ER_{W+R} were measured afterwards. For the Test 3, the roots with a relatively consistent diameter were selected and cut into 5 cm lengths. The EC_{root} and ER_{root} were measured for 12 individual root samples. At the same time, 15 roots from the same batch of roots were added into the soil. Similarly, we measured EC_{soil} and ER_{soil} for a random amount from the sieved soil before adding roots and did the measurements again for another amount of soil from the same sieved soil. The EC before and after root adding was measured using an LCR-meter (TH2826 with an accuracy of 0.1 %; Tonghui Electronics Co., Ltd., Changzhou, China) at 500 different frequencies linearly spaced from 20 Hz to 500 kHz with two stainless steel plates (for Tests 1 and 2, 10 cm long, 5.6 cm wide, spaced 5.8 cm apart, and 1 mm thick; for Test 3, 10 cm long, 8 cm wide, spaced 11.8 cm apart, and 1 mm thick) used as electrodes (Supplementary Fig. 1B). The relative permittivity and conductivity of the roots were calculated in Eqs. (16) and (17), respectively (Zhao, 2008).

$$\varepsilon = \frac{ECd}{s\varepsilon_0}, \quad (16)$$

where d is the distance between electrodes (root length) and s is the area of electrodes (root cross section area)

$$k = \frac{d}{sER}, \quad (17)$$

where ER represents electrical resistance.

Additional wheat roots at the jointing stage were collected in the field to test the correlation between EC_{M+R} and root traits. The cleaned roots with different volumes (0.117–0.381 cm^3) were separately placed into 28 plastic boxes (length of 12 cm, width of 8.6 cm, and height of 5 cm). Then, 500 mL of water was added to measure EC_{W+R}. Four plots containing only water were used as blank control. We used the LCR-meter (TH2817B + with an accuracy of 0.1 %, Tonghui Electronics Co., LTD, Changzhou, China) to measure EC_{W+R} at 50 Hz, 60 Hz, 100 Hz, 120 Hz, 1 kHz, 10 kHz, 20 kHz, 40 kHz, 50 kHz and 100 kHz. The wheat roots at the heading stage were collected again in the field to verify the relationship of EC_{S+R} with root traits. After rinsing the roots, 12 groups of fresh roots with different volumes (0.215–0.578 cm^3) were placed in plastic boxes as described above but filled the box with sieved soil and saturated with water. Again, four plots with bare soil were set up as blank control. EC_{S+R} was measured similarly as EC_{W+R}.

3.1.2. Root immersing and burying experiments for the two-phase model verification

Field grown maize (*Zea mays* L.) roots (15 days after sowing) were excavated with a shovel and washed with tap water gently. Fresh roots (60 g) were evenly separated into six portions and were placed into plastic boxes (length in 12 cm, width in 8.6 cm and height in 5 cm) filled with tap water. Another six plots filled with tap water but without roots were treated as blank control. The measurement processes of EC_{water} and EC_{W+R} were consistent with those of previous root addition experiments (Supplementary Fig. 1B). The medium was changed from tap water to sieved soil at saturated water content (0.32 g g^{-1}), and the EC_{soil} and EC_{S+R} were measured again following the same protocol as EC_{water} and EC_{W+R}.

A root burying experiment using maize roots (Table 1, 37 days after sowing) was conducted to explore the effect of root additions on EC_{S+R} under different soil textures and water additions. Sand with three different soil water contents (SWC) (0.1 g g^{-1}, 0.2 g g^{-1} and 0.25 g g^{-1}) and field sieved soil with four different SWCs (0.05 g g^{-1}, 0.1 g g^{-1}, 0.2 g g^{-1} and 0.25 g g^{-1}) were prepared using dry sand and dry soil, respectively. The same plastic pots mentioned above were used, and 20 g of fresh roots were buried in the sand and field soil. Each soil texture/water content combination was replicated six times. Similarly, another six replications of each soil texture/water content combination were created without root additions to serve as a control. The soil was then compacted to a bulk density of 1.4 g cm^{-3} and EC was measured as aforementioned in the seedling maize root burying experiment.

3.2. Experiment 2: Root washing-free experiment for model application

Maize roots at the grain-filling stage were collected using a soil auger (10 cm in diameter). Soil samples with roots were taken down to 50 cm with 10 cm increment, and a total of 150 soil samples were obtained. Next, 620 g of soil was weighed and added into the plastic box. The EC_{S+R} and ER_{S+R} in the plastic box were measured in the same way as in the root addition experiments after soil was saturated with water. The root system was cleaned and root volume was measured. Due to loss of several roots during the cleaning process, a total of 140 complete samples were obtained in this study. Among them, 90 were used for building the empirical model with the regression relationships between root volume and EC_{S+R}. The remaining 50 samples were used to test the model results. This experiment was used to testify if the EC_{S+R} method can be used to measure root volume without washing out roots in the traditional way.

3.3. Experiment 3: Soil pot application experiment

In the first pot experiment (Pot 1), five wheat cultivars (i.e., Gaoyou 2018, Nongda 212, Zhongmai 175, Shiyou 20 and Jimai 22) were planted with two water treatments of dry (0.16 g g^{-1}) and deficit (0.21 g g^{-1}) soil with seven replicates (Table 1 and Supplementary Fig. 1C). Then, 2 kg of sieved soil (the initial soil moisture content was 0.10 g g^{-1}) was added into a cylindrical pot (16 cm in height and 14 cm in diameter). The soil bulk density was compacted to 1.1 g cm^{-3}, and 400 mL of tap water was irrigated. The next day, six seeds were sowed in each pot, and one week after emergence, three wheat seedlings were left in each pot. The experiment was performed in a greenhouse with 12 h of light and 12 h of darkness. The average temperature was 25 °C during day and 15 °C during the night. No water treatment was applied during the first three weeks after emergence, and water was replenished every three days at a rate of 67 mL/day. The dry and deficit treatments were weighed every 7 days and 3 to 4 days, respectively, after which water was replenished to the designed soil moisture.

In the second soil pot experiment (Pot 2), six replicates of eight wheat cultivars (i.e., Gaoyou 2018, Nongda 212, Zhongmai 175, Shiyou 20, Jimai 22 Jimai 38, Jinmai 47 and Shixin633), were grown under two water treatments: wet soil (0.32 g g^{-1}) and dry soil (0.15 g g^{-1}) conditions. Other treatments were consistent with Pot 1. Another six pots without plants received the same water supply and were used as controls. One week after emergence, plants were thinned to 4 in 32 pots, to two plants in eight pots and to one in eight pots for each water treatment. The dry pots were irrigated every 7 days, and the wet treatment pots were irrigated every 3 to 4 days, according to the designed SWC.

The TH2817B + LCR-meter was used to measure EC_{S+R} for both soil pot experiments (Supplementary Fig. 1C). For Pot 1, EC_{S+R} and ER_{S+R} were measured before and after rewatering. For Pot 2, EC_{S+R} was measured at 20 days, 26 days, 31 days, 35 days, 38 days, 41 days, 44 days after sowing for wet treatment. Stainless steel rods with a diameter of 3 mm and a length of 18 cm were used as electrodes, which inserted 12 cm deep into the soil and spaced 13 cm apart. SWC was also measured at the same time as the final EC_{S+R} measurement.

3.4. Experiment 4: Field application experiment

Finally, to test whether EC_{S+R} measured the root depth distribution in the field (Table 1 and Supplementary Fig. 1D), a trench was dug in a maize field at the heading stage. The trench measured 120 cm long, 30 cm deep, and 60 cm wide. A TH2826 LCR-meter was used to measure EC_{S+R} at 500 frequencies (20–500 kHz) with stainless steel plates as electrodes. The electrodes, measuring 10 cm in length, 8 cm in width, and 1 mm in thickness, were inserted 8 cm into the undisturbed soil and spaced 10 cm apart. Measurements were taken at 12 locations in the horizontal direction and 3 depth intervals (0–10, 10–20 and 20–30 cm) in the vertical direction (the volume of soil sample is 10 × 10 × 8 cm^3), resulting in a total of 36 data points. After the measurement, a knife was used to cut and remove sections of soil (10 × 10 × 8 cm^3) to collect the roots from the volume. After completing the EC measurements, root samples were processed as the soil pot experiment and root traits were determined accordingly.

3.5. Root measurements

The soil was washed through a stainless-steel sieve with a 0.425 mm mesh to collect the roots, which were then stored in a − 20 °C freezer. Root samples were further cleaned in the laboratory by manually removing debris and scanned (Epson Expression 12000XL, USA) at a resolution of 600 dpi. Root parameters such as root length, root surface area and root volume were analyzed by using WinRhizo software (ver. 2019a, Reagent Instruments Inc., Quebec, Canada). Then the roots were oven dried at 75 °C until they reached a constant weight. Root volume, biomass and length were highly correlated with each other, though root volume is the primary basis for our EC hypothesis as described in the introduction.

3.6. Statistical analysis

R (version 4.0.4) was used to perform statistical analysis and to plot the data (R Core Team, 2021). Before conducting variance analysis, the data were assessed for normality and homogeneity of variance. Linear fitting was performed using the lm() functions. The *t*-test was utilized to compare mean differences and examine whether the correlation coefficient was zero. The change in EC (EC change rate) was derived from the following Eq. (18):

$$ECchangerate = \frac{meanEC(f, root) - meanEC_m(f)}{meanEC_m(f) \times RFM} \times 100\%. \quad (18)$$

In the formula, mean EC (f, $root$) and mean EC_m (f) are mean EC with roots and without roots at f measurement frequency, respectively; RFM is root fresh mass.

The relative error was used to evaluate the validity of the formula for calculating root volume.

$$Relativeerror = \frac{|Calculatedrootvolume - measuredrootvolume|}{measuredrootvolume} \times 100\%. \quad (19)$$

4. Results

4.1. Model validation

The two assumptions for transferring Eq. (13) to Eq. (14) were verified in a series of root burying/immersing experiments (Fig. 1A,B). It was found that the relative permittivity of roots was 200 and 300 times greater than that of soil and water under high frequencies of 30 kHz–60 kHz, respectively, and the values of root relative permittivity multiplied by medium electrical conductivity were also much greater than those of medium relative permittivity multiplied by root conductivity (more than 59 and 73 times for soil and water under frequencies of 30 kHz–60 kHz, respectively). These results show that the simplification of Eq. (13) is reasonable.

From Eqs. (14) and (15) it is known that EC_{M+R} is affected by root volume, root relative permittivity, root electrical conductivity, medium relative permittivity, and medium electrical conductivity. In order to verify whether Eqs. (14) and (15) can be used to calculate root volume in theory, fresh wheat nodal roots were used to determine root EC (EC_{root}, hereafter specifically indicates the root electrical capacitance, which is different from the aforementioned EC_{system}) and root ER (ER_{root}) in the laboratory. Here, three methods for measuring these electrical parameters were compared. The first method involves conducting comprehensive measurements for both roots and medium. The second method entails incomplete measurements for roots but complete measurements for the medium. The third method involves incomplete measurements for both roots and medium. The results showed that the relative error between the calculated root volume and the measured root volume varied with frequency, and it reached to the minimal levels at two ranges of frequency of 3–50 kHz and 210–440 kHz (Fig. 1C–G). The minimum relative errors between calculated root volume with Eq. (14) and measured root volume for three methods were 0.15 % (0.06 % for the soil medium and 0.23 % for the water), 6.1 % and 15.6 %, respectively. Similarly, the minimal estimation errors when using Eq. (15) to calculate root volume were 0.13 % (0.2 % for the soil medium and 0.05 % for the water), 5.6 % and 16.0 %, respectively. It was evident that accurate measurements of the required electrical parameters ensured satisfactory estimations. Additionally, the frequency range that yielded mean errors of less than 15 % with Eq. (15) was broader than that of Eq. (14) (increasing from 120 to 136 frequencies for soil and from 130 to 149 frequencies for water in Test 1, and from 139 to 272 frequencies for Test

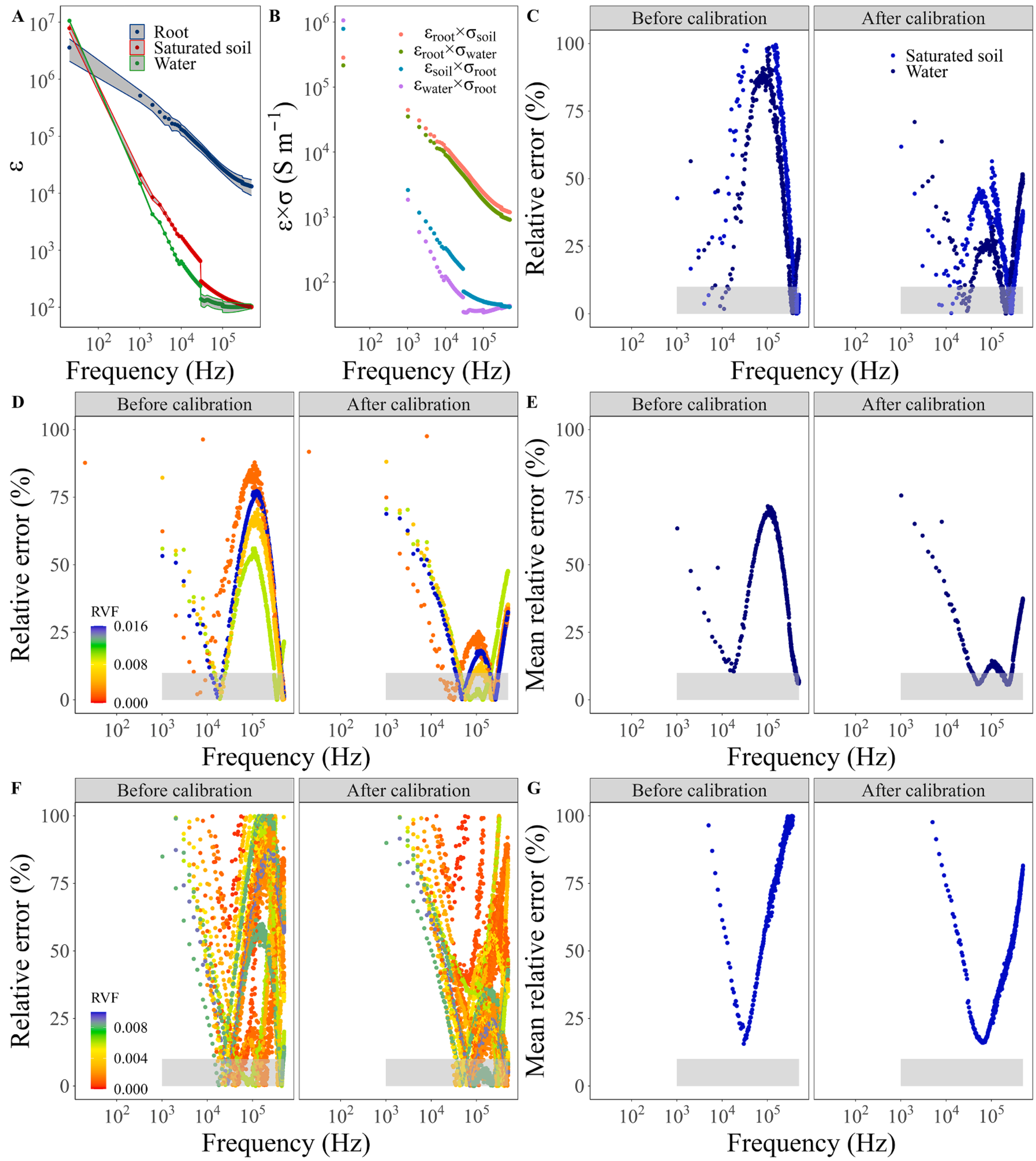

Fig. 1. The relative permittivity (A), the value of relative permittivity multiplied by conductivity (B), and the changes of the error between calculated and measured root volume with frequencies (C–G). (C) EC_{medium} and ER_{medium} were measured on fixed soil and water; EC_{root} and ER_{root} were measured separately for each root. (D and E) EC_{medium} and ER_{medium} were measured on water, and EC_{root} and ER_{root} were measured for several random root samples. (F and G) EC_{medium} and ER_{medium} were measured on a sampling soil from a large amount of sieved soil, and EC_{root} and ER_{root} were measured for several samples from a large set of fresh samples. The shaded parts in (A) represent the 95% confidence interval. The shaded area in (C–G) indicates a relative error of less than 10%. RVF represents root volume fraction.

2, as shown in Fig. 1C and E). A regression analysis was further performed for the Test 3 to compare the calculated root volume and the measured root volume before and after calibration with the shape factor (corresponding frequencies were 30 kHz and 64 kHz, respectively) (Supplementary Fig. 2). The fitting line of calculated root volume after calibration and measured root volume almost completely coincided with the 1:1 line. Therefore, Eq. (15) tends to be more suitable for estimating root volume than Eq. (14).

Another way to validate the two-phase theoretical model was evaluated. According to Eq. (15), when the medium without roots is uniform, root volume should be linearly and positively correlated with EC_{M+R} as roots will domain the changes of EC_{M+R}. To verify that, fresh roots with different mass values with known root volume were buried in the wet soil or immersed in the water. The results showed that as the measurement frequency increased, EC_{M+R} buried in soil and immersed in water became significantly ($P < 0.05$, Fig. 2) greater than EC_{medium}. Adding per gram of roots maximally increased EC_{W+R} by 44.9 % while the maximum increase in EC_{S+R} was 29.3 % in the sand and 22.9 % in field soil (Fig. 2A). All these highest increments were observed at around 30 kHz. Positive correlations between root volume and high-frequency EC_{M+R} (Fig. 3) were observed, in line with the linear negative correlation between root systems size and electrical impedance magnitude at high frequency in uniform water conditions reported in Basak and Wahid, (2022). In particular, when the measurement frequency was 8 kHz–84 kHz, the correlation coefficient was greater than 0.96 ($P < 0.0001$). Overall, the two-phase theoretical model worked well in the

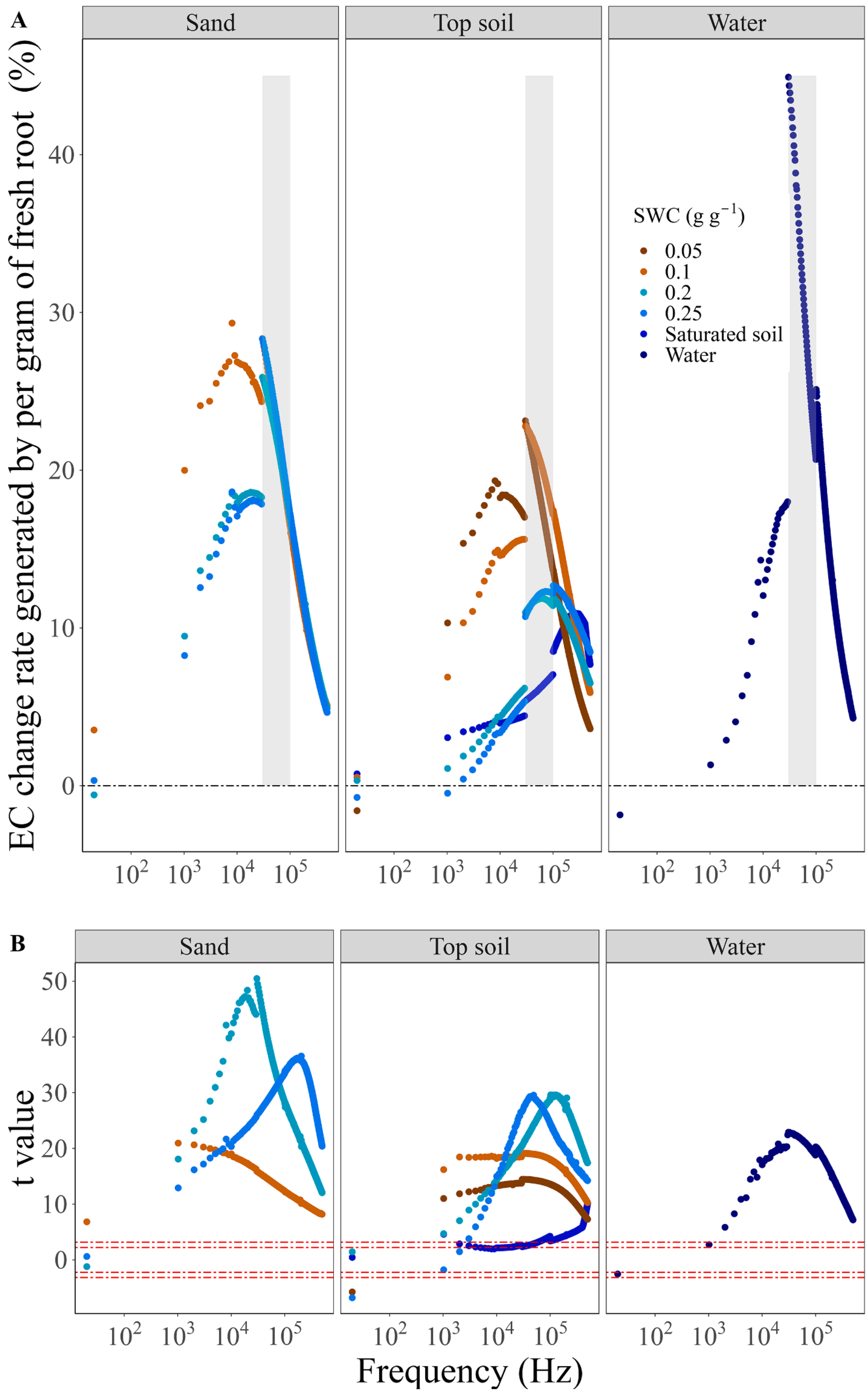

Fig. 2. Effects of fresh roots on medium electrical capacitance (EC, A) and the corresponding two-tailed test results of mean values with and without roots in the medium (B). The shaded area represents the frequency ranges from 30 kHz to 100 kHz. The two red lines above 0 represent significant levels of 0.05 and 0.01, respectively. SWC represents soil water content.

control conditions.

4.2. Model applications

As previously mentioned, accurate measurement of the five required electrical parameters allows for a satisfactory estimation of root volume. However, obtaining these electrical parameters *in situ*, except for EC_{S+R} and ER_{S+R}, may present practical challenges. To maximally consider both the theoretical and practical parts, Eq. (15) was further simplified. First, root electrical parameters were treated as constant and $\Phi \ll 1$. Second, ER_{S+R} was used to represent soil electrical conductivity and soil permittivity, as roots have minimal effects on ER_{S+R}, and that soil conditions, such as water content, and salinity, have opposite effects on EC_{soil} and ER_{soil}, which suggests there is a negative correlation between EC_{soil} and ER_{soil} (Supplementary Figs. 3 and 4). Then, the following equations can be derived.

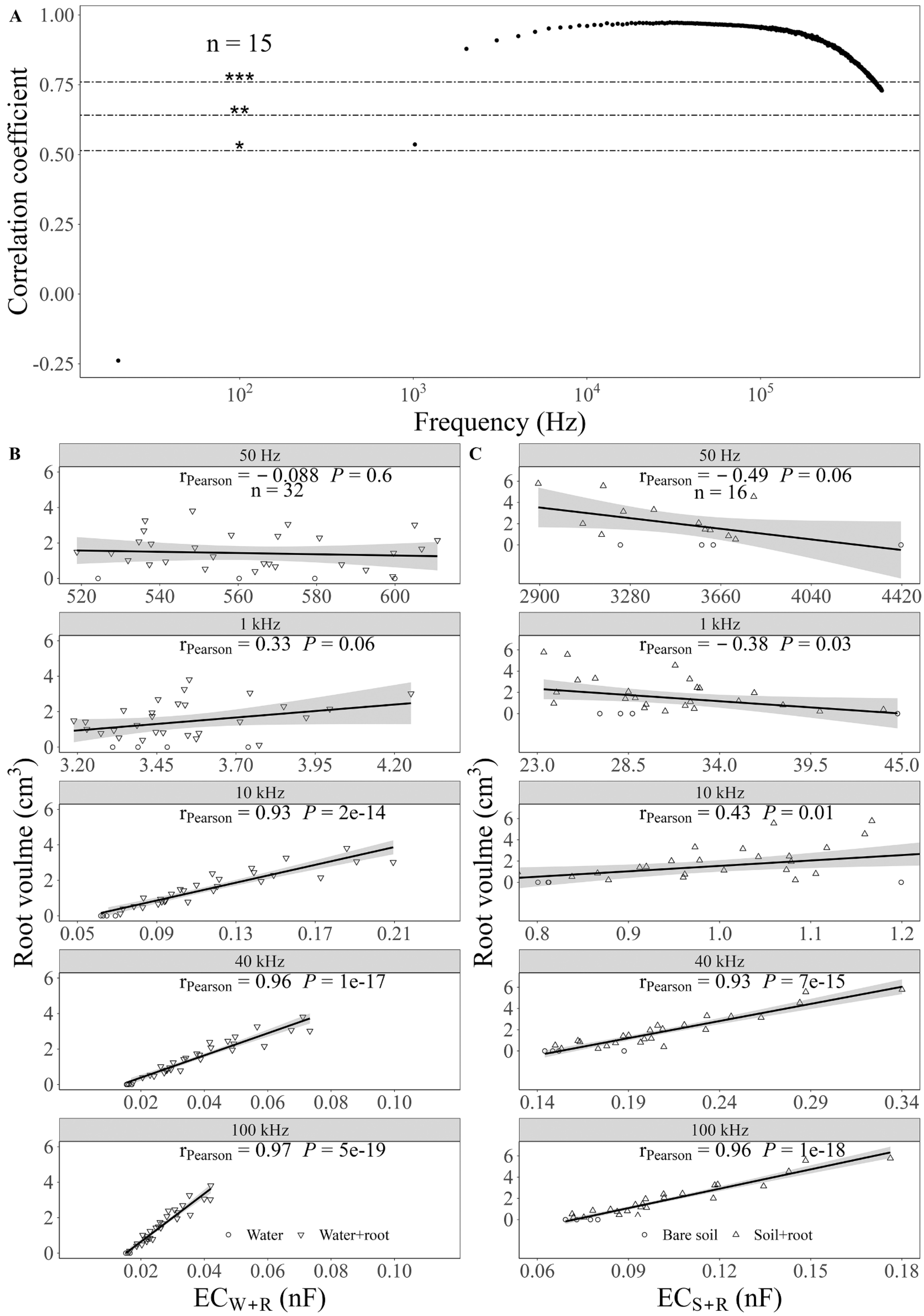

Fig. 3. The relationships between root volume and bulk medium electrical capacitance for the wheat root addition experiments. EC_{S+R} indicates the electrical capacitance of soil with roots, and EC_{W+R} indicates the electrical capacitance of water with roots. *, **, and *** represent the significance levels at 0.05, 0.01, and 0.001, respectively.

$$\varepsilon(\omega) \approx \frac{3}{2}\Phi\left[\frac{9\varepsilon_i k_m^2}{(2k_m+k_i)^2+\omega^2\varepsilon_0^2\varepsilon_i^2}\right]+\varepsilon_m, \tag{20}$$

$$ER_{soil} \approx ER_{S+R}, \tag{21}$$

$$EC_{soil} = \frac{\gamma_1}{ER_{soil}} + \gamma_2 \approx \frac{\gamma_1}{ER_{S+R}} + \gamma_2, \tag{22}$$

$$\Phi = \frac{RV}{V_{soil}} = \frac{RV}{ds}, \tag{23}$$

where RV and V_{soil} represent the root volume and measured soil volume, respectively. γ_1 and γ_2 are the parameters to be fitted.

Combining Eqs. (16)–(23) can form a new equation for calculating root volume. To facilitate expression, six coefficients namely β_1, β_2, β_3, β_4, β_5, and β_6 were donated and K was denoted as the constant term. Then, Eq. (24) can be derived as follows:

$$RV = \beta_1 EC_{S+R} \times ER_{S+R}^2 + \beta_2 EC_{S+R} \times ER_{S+R} + \beta_3 EC_{S+R} + \beta_4 ER_{S+R}^2 + \beta_5 ER_{S+R} + \frac{\beta_6}{ER_{S+R}} + K, \quad (24)$$

where β_1, β_2, β_3, β_4, β_5, β_6, and K are expressed as follows:

$$\beta_1 = \frac{2}{27}\left(k_i s^2 + \omega^2 \varepsilon_0^2 \varepsilon_i^2\right), \quad (25)$$

$$\beta_2 = \frac{8}{27} V_{soil} k_i, \quad (26)$$

$$\beta_3 = \frac{8}{27} d^2, \quad (27)$$

$$\beta_4 = -\gamma_2\left(k_i s^2 + \omega^2 \varepsilon_0^2 \varepsilon_i^2\right), \quad (28)$$

$$\beta_5 = -4V_{soil}\gamma_2 - \gamma_1\left(k_i s^2 + \omega^2 \varepsilon_0^2 \varepsilon_i^2\right), \quad (29)$$

$$\beta_6 = -4d^2\gamma_1, \quad (30)$$

$$K = -4V_{soil}\gamma_1 - 4d^2\gamma_2. \quad (31)$$

The close correlation between high-frequency EC_{M+R} and root volume indicates that high-frequency EC_{M+R} within an empirical model may be also applicable to specifically predict root volume (Fig. 3). Next, theoretical and empirical models were tested in three applications (Fig. 4).

Root cleaning process is the most time-consuming part for the traditional root measurement methods (such as soil coring), during which part of fine root information is easily missing. To resolve this issue, we proposed a rapid root size (volume) measurement to replace root cleaning process and we named it a root washing-free method. For the specific operation process, see the Materials and Methods section. The 90 soil samples containing maize roots were used to build the empirical regression model, and the other 50 samples were used to test the model (Fig. 4A and B). The RMSE of the modeling data set and the test date set was 0.46 cm^3 and 0.36 cm^3, respectively, indicating that the EC_{S+R} performed well in predicting root volume. In addition, the residual distribution followed a normal distribution (Supplementary Fig. 5), indicating that the errors during modeling and testing were caused by random factors. Therefore, directly building the empirical model with high-frequency EC_{S+R} can be used to predict root volume, which shows the high potential to replace root cleaning process for root size measurements.

Moving forward, EC_{S+R} was applied in soil pots and field-grown conditions to test whether it measures root volume *in situ*. High-frequency EC_{S+R} significantly correlated with root volume in both applications, particularly for the field applications. The best empirical correlation at 71 kHz ($r = 0.91$, $P < 0.0001$, $n = 36$, RMSE $= 1.52$ cm^3) between EC_{S+R} and root volume in the field was used to calculate the difference between measured and estimated root volume (Fig. 4D and E). The mean error across all depths was 9.2 % with depth-specific means of 3.8 %, 11.6 %, and 12.2 % at 10 cm, 20 cm and 30 cm, respectively. However, the correlation between root volume and high-frequency EC_{S+R} was weaker in the soil pot experiments (Fig. 4E and Supplementary Fig. 6) possibly due to the large soil heterogeneity caused by root uptake water and ions (Supplementary Fig. 7). From Eq. (15), it can be seen that EC_{S+R} is affected not only by roots but also by soil conductivity, and there is an interaction effect of EC_{S+R} and soil conductivity on root volume. It was shown that ER_{S+R} was not largely affected by roots in the root burying experiments. This was also evidenced by the increasing ER_{S+R} over time in the second soil pot experiment (because roots themselves should cause ER_{S+R} in a decreased trend), but it had a close relation with soil water and ion content (Supplementary Figs. 3, 7, and 8). Therefore, ER_{S+R} may be used to exclude the soil background information. Then, Eq. (24) was used to fit the model, and the results showed that $EC_{S+R} \times ER_{S+R}^2$ was closely related with root volume in all the soil pot experiments (Table 2). After calibration with ER_{S+R} at 100 kHz, the correlation coefficients increased from -0.08 to 0.52 under dry treatment and increased from 0.008 to 0.63 under deficit treatment in Pot 1. Similarly, the correlation coefficients increased from -0.46 to 0.83 under dry treatment, and from 0.5 to 0.93 under wet treatment in Pot 2 (Fig. 4E, G, H). The correlation coefficients of overall fitting was 0.89 in Pot 1 and 0.92 in Pot 2.

The results above indicated that high-frequency (30–100 kHz) EC_{S+R} within an empirical model can generally provide accurate estimates of root volume. However, in cases where the empirical model does not perform optimally, the two-phase model can be used to enhance the empirical relationships. We demonstrated that when soil heterogeneity is significant, such as in the soil pot conditions, ER_{S+R} can be used to calibrate the relationship between EC_{S+R} and root volume. In addition, measuring the root electrical parameters for a few root samples can also improve the empirical relationships.

5. Discussion

5.1. Mechanism of high-frequency EC_{S+R} measuring root volume

To date, there are only a few reports proposing the application of a high-frequency EC_{medium} for measuring roots. Basak and Wahid (2022) observed a strong correlation between high-frequency impedance magnitude and carrot root size, and they also developed a cost-effective and high-speed data acquisition system. Wang et al. (2023) optimized the reconstruction algorithm for better imaging of the root zone of carrots and potatoes. Furthermore, the feasibility of using a high-frequency EC_{medium} to measure root size was verified by our previous work in wheat and corn grown under various conditions (Gu et al., 2023, a preprint on bioRxiv). However, all the previous work did not report the mechanism underlying high-frequency EC_{medium} measuring root size, which hinders its extensive use. This study tried to bridge this knowledge gap by presenting a theoretical model.

The conceptual model of the root-soil system polarization at different frequencies is shown in Supplementary Fig. 9. According to Eq. (15), the EC_{M+R} is influenced by the interaction between the root volume and the EC_{medium}. As known, the electrical conductivity of root is greater than that of soil and nutrient solution (Weigand and Kemna, 2017; Ehosioke et al., 2020; Basak and Wahid, 2022), which is in line with our results, indicating the electrical current easily enters the root. When the frequency is < 100 kHz, the root cell membrane is insulated compared to the cell liquid phase. As a result, the root cell can be regarded as a conductive sphere covered by an insulating layer (Fricke, 1931; Mancuso, 2012), and root membranes act as charge-storing dielectrics of the capacitor (Dalton, 1995). When the frequency increases to > 100 kHz, the interfacial polarization is induced in the cell membrane and other membrane systems (Zhao, 2008). Additionally, the relaxation time of the soil is about 0.11 s (Mary et al., 2017) and its characteristic relaxation frequency is about 1.4 Hz. Therefore, the soil is not fully charged when frequency is higher than 1.4 Hz. With the increase of frequency, the soil becomes less charged, which is represented by the decrease of soil permittivity. However, when the frequency is < 100 kHz, the cells will be fully charged (Zhao, 2008). Root epidermis and cell walls block the electrical charge movement and the charge accumulation leads to the interface polarization. Therefore, with the increase of frequency, the decrease of root relative permittivity is much smaller than that of soil

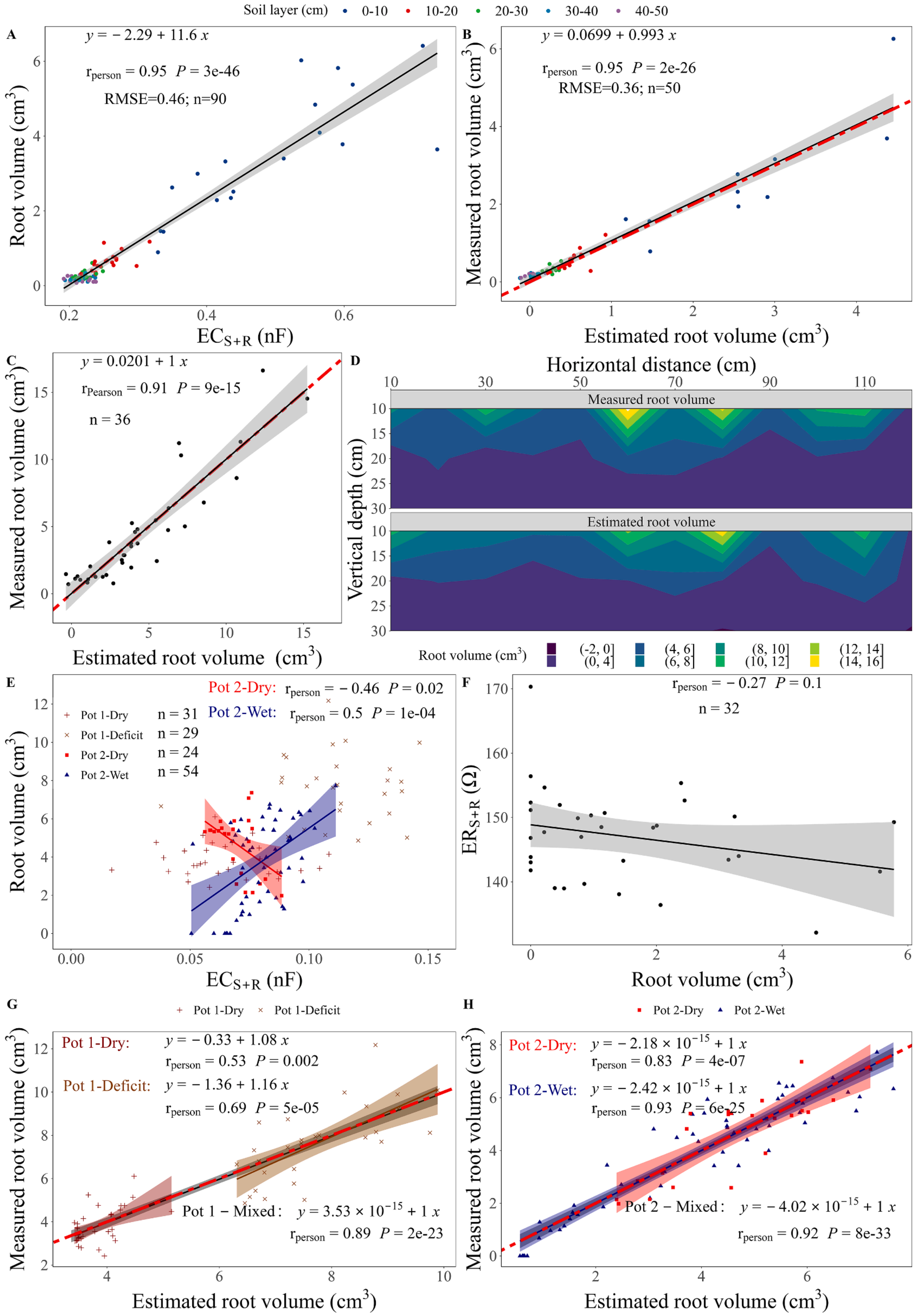

Fig. 4. The applications of using high frequency bulk soil capacitance to detect root volume. (A and B) The root washing-free measurements: (A) the modeling of the relationship between soil electrical capacitance with roots (EC_{S+R}) and root volume at different soil layers obtained in the summer maize field. (B) The testing of the model. (C and D) The application in the maize field experiment: (C) the relationship between measured and estimated root volumes and (D) the comparison between measured and estimated root volume distribution. (E) The relationship between EC_{S+R} and root volume in different soil pot experiments. (F) The relationship between soil electrical resistance with roots (ER_{S+R}) and root volume in wheat roots burying experiment. (G and H) The relationships between estimated root volume and measured root volume after calibration with ER_{S+R} for Pot 1 and Pot 2 experiments. RMSE represents the root mean square error and the shaded part represents the 95 % confidence interval. The dashed red line represents the 1:1 line.

Table 2
The relationships between root volume and $EC_{S+R} \times ER^2_{S+R}$.

Experiments	Treatment	Coefficient	Intercept	R^2	AIC	*P*	Sample size
Pot 1	Deficit	1.28×10^{-4}	6.14	0.40	108	**	29
	Dry	6.12×10^{-5}	3.36	0.27	79	**	31
	Mixed	2.4×10^{-4}	5.20	0.29	276	**	60
Pot 2	Dry	2.67×10^{-4}	−0.92	0.70	66	**	24
	Wet	2.3×10^{-4}	−1.06	0.87	132	**	54
	Mixed	2.3×10^{-4}	−0.87	0.80	213	**	78

Note: EC_{S+R}, soil electrical capacitance; ER_{S+R}, soil electrical resistance with roots; AIC, Akaike information criterion. ** indicates significant coefficient at $P = 0.01$.

relative permittivity. As a result, the root permittivity is much higher than that of the soil (Fig. 1). Thus, EC_{S+R} at high frequency is linearly and positively correlated with root volume.

The polarization of root-soil system is not only affected by frequency, but also by root physiological state and soil environment. Under stress conditions, the increased permeability of the cell membrane leads to a decrease in the accumulation of charge on the cell membrane, which ultimately leads to a decrease in the relative permittivity of the root system (Zhao, 2008). This was supported by the wheat roots immersing experiments where roots from different water treatments represent different root vigor (Supplementary Fig. 10). SWC, soil ion content, soil bulk density, surface-charged colloid particles (i.e., clay minerals), and organic-mineral complexes can significantly affect EC_{S+R} (Li et al., 2005; Fares and Polyakov, 2006; Postic and Doussan, 2016, Cseresnyés et al., 2017). However, the reduction of high-frequency EC_{S+R} due to root absorption can be masked by root polarization (Supplementary Fig. 8A). This may partially explain why the correlations between high-frequency EC_{S+R} and electrical conductivity or ion concentration were not significant in the soil pot experiment (Supplementary Fig. 7).

5.2. Future perspectives

Root volume correlates with other root size traits, such as root length and root biomass. The reliable estimation of root volume achieved through the three application tests using high-frequency EC_{S+R} suggests its potential for measuring other root traits, including root 3D distribution and dynamic changes in root growth. This is particularly advantageous for taproot systems, which are difficult to assess with minirhizotron techniques. Compared with EC_{system}, EC_{S+R} does not have the issue of current leakage in the root system which enables EC_{S+R} to measure deep roots. High-frequency EC_{S+R} also shows the advantage over the low-frequency EC_{S+R} in both the mechanism and application aspects for detecting root size. Thus, we foresee that high-frequency EC_{S+R} with the help of the theoretical model opens a new door to develop nondestructive and noninvasive root phenotyping technique. To enhance the feasibility of EC_{S+R}, further research is needed to characterize the influence of the root physiological state, soil environment, and measurement method (e.g., electrode material, shape, and distance) on the detecting accuracy. Even if the equipment used in this study is not the most advanced (<$3900), it can still give us a reliable assessment of root traits. We propose that with the development and application of new advanced equipment, the measuring accuracy should be improved further. For example, if a new equipment can measure the five electrical parameters in the two-phase model, root volume and other root size traits will be accurately detected.

6. Conclusions

In conclusion, a theoretical model is presented in this study to enable high-frequency EC_{S+R} to measure root volume. The theoretical model was validated under indoor control conditions, and as long as the required electrical parameters are accurately measured, the developed model can estimate root volume with high precision. For the application purpose, the empirical model with high-frequency EC_{S+R} can be used to predict root volume under relatively uniform soil conditions such as in the root washing-free measurements and the field. When the soil is in high heterogeneity, the combination of theoretical and empirical models allows for accurate and robust *in situ* measurement of root volume such as in the soil pots. Moreover, the high-frequency EC_{S+R} approach enables direct measurement of other root size traits. We anticipate that the integration of the newly available equipment with this novel root prediction model will establish EC_{S+R} as a widely adopted root phenotyping technique in the future.

CRediT authorship contribution statement

Huijie Gu: Conceptualization, Data curation, Investigation, Methodology, Visualization, Writing – original draft, Writing – review & editing. **Imre Cseresnyés:** Methodology, Writing – original draft, Writing – review & editing. **John R. Butnor:** Methodology, Writing – original draft, Writing – review & editing. **Baoru Li:** Investigation, Writing – original draft. **Hongyong Sun:** Funding acquisition, Methodology, Writing – original draft, Writing – review & editing. **Xiying Zhang:** Methodology, Writing – original draft, Writing – review & editing. **Yang Lu:** Funding acquisition, Methodology, Writing – original draft. **Xiuwei Liu:** Conceptualization, Data curation, Funding acquisition, Investigation, Methodology, Writing – original draft, Writing – review & editing.

Declaration of competing interest

The authors declare the following financial interests/personal relationships which may be considered as potential competing interests: Xiuwei Liu reports financial support was provided by the National Key R&D Program of China. Yang Lu reports financial support was provided by Key Research & Development Program of Hebei Province.

Data availability

Data will be made available on request.

Acknowledgments

The authors thank Hanbing Jiang, Shiming Duan, Weishuang Feng, and Zhaoliang Mei for helping with field sampling and providing assistance in processing root samples. We thank LetPub (www.letpub.com) for linguistic assistance and pre-submission expert review. This study was funded by the National Key R&D Program of China (2022YFD1300801), the Key Research & Development Program of Hebei Province (21327201D) and the National Natural Science Foundation of China (32370434).

Appendix A. Supplementary data

Supplementary data to this article can be found online at https://doi.org/10.1016/j.geoderma.2024.116773.

References

Basak, R., Wahid, K.A., 2022. An in situ electrical impedance tomography sensor system for biomass estimation of tap roots. Plants. 11, 1713. https://doi.org/10.3390/plants11131713.

Chloupek, O., 1972. The relationship between electric capacitance and some other parameters of plant roots. Biol. Plantarum. 14, 227–230. https://doi.org/10.1007/BF02921255.

Cimpoiasu, M.O., Kuras, O., Pridmore, T., Mooney, S.J., 2020. Potential of geoelectrical methods to monitor root zone processes and structure: a review. Geoderma 365, 114232. https://doi.org/10.1016/j.geoderma.2020.114232.

Cseresnyés, I., Kabos, S., Takács, T., Végh, K.R., Vozáry, E., Rajkai, K., 2017. An improved formula for evaluating electrical capacitance using the dissipation factor. Plant and Soil 419, 237–256. https://doi.org/10.1007/s11104-017-3336-4.

Dalton, F.N., 1995. In-situ root extent measurements by electrical capacitance methods. Plant and Soil 173, 157–165. https://doi.org/10.1007/BF00155527.

Debye, P., 1912. Some results of kinetic theory of isolators. (preliminary announcement). Physikalische Zeitschrift. 13, 97–100.

Ehosioke, S., Nguyen, F., Rao, S., Kremer, T., Placencia-Gomez, E., Huisman, J.A., Kemna, A., Javaux, M., Garre, S., 2020. Sensing the electrical properties of roots: a review. Vadose Zone J. 19, e20082.

Ellis, T., Murray, W., Kavalieris, L., 2013a. Electrical capacitance of bean (Vicia faba) root systems was related to tissue density-a test for the dalton model. Plant and Soil 366, 575–584. https://doi.org/10.1007/s11104-012-1424-z.

Ellis, T., Murray, W., Paul, K., Kavalieris, L., Brophy, J., Williams, C., Maass, M., 2013b. Electrical capacitance as a rapid and non-invasive indicator of root length. Tree Physiol. 33, 3–17. https://doi.org/10.1093/treephys/tps115.

Fares, A., Polyakov, V., 2006. Advances in crop water management using capacitive water sensors. Adv. Agron. 90, 43–77. https://doi.org/10.1016/S0065-2113(06)90002-9.

Fricke, H., 1931. The electric conductivity and capacity of disperse systems. Phys. 1, 106–115. https://doi.org/10.1063/1.1744988.

Gan, Y., Liu, L., Cutforth, H., Wang, X., Ford, G., 2011. Vertical distribution profiles and temporal growth patterns of roots in selected oilseeds, pulses and spring wheat. Crop Pasture Sci. 62, 457–466. https://doi.org/10.1071/CP10406.

Gu, H., Cseresnyés, I., Butnor, J.R., Li, B., Mary, B., Sun, H., Zhang, X., Lu, Y., Liu, X., 2023. High frequency soil polarization can phenotype crop roots noninvasively. bioRxiv. 2023.01.12.523853; doi: https://doi.org/10.1101/2023.01.12.523853.

Gu, H., Liu, L., Butnor, J.R., Sun, H., Zhang, X., Li, C., Liu, X., 2021. Electrical capacitance estimates crop root traits best under dry conditions-a case study in cotton (Gossypium hirsutum L.). Plant and Soil 467, 549–567. https://doi.org/10.1007/s11104-021-05094-6.

IUSS Working Group, 2015. International soil classification system for naming soils and creating legends for soil maps. World Soil Resources Reports 106, FAO, Rome.

Karlova, R., Boer, D., Hayes, S., Testerink, C., 2021. Root plasticity under abiotic stress. Plant Physiol. 187, 1057–1070. https://doi.org/10.1093/plphys/kiab392.

Kessouri, P., Furman, A., Huisman, J.A., Martin, T., Mellage, A., Ntarlagiannis, D., Bücker, M., Ehosioke, S., Fernandez, P., Flores-Orozco, A., et al., 2019. Induced polarization applied to biogeophysics: recent advances and future prospects. Near Surf. Geophys. 17, 595–621. https://doi.org/10.1002/nsg.12072.

Kuang, W., Nelson, S.O., 1998. Low-frequency dielectric properties of biological tissues: A review with some new insights. T Asabe. 41, 173–184. https://doi.org/10.13031/2013.17142.

Li, Y., Wang, Y., Zhao, P., Wang, N., Huang, L., Wang, Z., 2020. Development and Experiment on Electrical Impedance Tomography System for Plant Root Zone. Transactions of the Chinese Society for Agricultural Machinery, 51, 349-355. https://doi:10. 6041/j. issn. 1000-1298. 2020. S1. 041.

Li, X., Lei, T., Wang, W., Xu, Q., Zhao, J., 2005. Capacitance sensors for measuring suspended sediment concentration. Catena 60, 227–237. https://doi.org/10.1016/j.catena.2005.01.001.

Liao, A., Zhou, Q., Zhang, Y., 2015. Application of 3D electrical capacitance tomography in probing anomalous blocks in water. J. Appl. Geophys. 117, 91–103. https://doi.org/10.1016/j.jappgeo.2015.03.030.

Lynch, J.P., 2013. Steep, cheap and deep: an ideotype to optimize water and N acquisition by maize root systems. Ann Bot-London. 112, 347–357. https://doi.org/10.1093/aob/mcs293.

Lynch, J.P., 2019. Root phenotypes for improved nutrient capture: an underexploited opportunity for global agriculture. New Phytol. 223, 548–564. https://doi.org/10.1111/nph.15738.

Mancuso, S., 2012. Measuring roots: An updated approach. Springer-Verlag, Berlin Heidelberg, Springer Science & Business Media.

Mary, B., Abdulsamad, F., Saracco, G., Peyras, L., Vennetier, M., Meriaux, P., Camerlynck, C., 2017. Improvement of coarse root detection using time and frequency induced polarization: from laboratory to field experiments. Plant and Soil 417, 243–259. https://doi.org/10.1007/s11104-017-3255-4.

Maxwell, J.C., 1891. A Treatise on Electricity & Magnetism. Clarendon Press, Oxford UK.

Peruzzo, L., Chou, W., Wu, Y.X., Schmutz, M., Mary, B., Wagner, F.M., Petrov, P., Newman, G., Blancaflor, E.B., Liu, X., et al., 2020. Imaging of plant current pathways for non-invasive root Phenotyping using a newly developed electrical current source density approach. Plant and Soil 450, 567–584. https://doi.org/10.1007/s11104-020-04529-w.

Postic, F., Doussan, C., 2016. Benchmarking electrical methods for rapid estimation of root biomass. Plant Methods 12, 1–11. https://doi.org/10.1186/s13007-016-0133-7.

R Core Team, 2021. A language and environment for statistical computing. R Foundation for Statistical computing, Vienna, Austria http://www.R-project.org/.

Rajkai, K., Végh, R.K., Nacsa, T., 2005. Electrical capacitance of roots in relation to plant electrodes, measuring frequency and root media. Acta Agron. Hung. 53, 197–210. https://doi.org/10.1556/AAgr.53.2005.2.8.

Tsukanov, K., Schwartz, N., 2020. Relationship between wheat root properties and its electrical signature using the spectral induced polarization method. Vadose Zone J. 19, e20014.

Tsukanov, K., Schwartz, N., 2021. Modeling Plant Roots Spectral Induced Polarization Signature. Geophys. Res. Lett. 48, e2020GL090184 https://doi.org/10.1029/2020GL090184.

Tsukanov, K., Schwartz, N., 2023. The influence of roots on soil's electrical signature. Rhizosphere-Neth. 25 (100670) https://doi.org/10.1016/j.rhisph.2023.100670.

Wagner, K., 1914. Explanation of the dielectric fatigue phenomenon on the basis of Maxwell's concept. Arkiv Für Electrotechnik. 2, 371–387.

Wang, N., Li, Y., Huang, L., Wang, Z., Zhao, P., 2023. Multi-frequency complex conductivity sparse imaging of plant root zone based on space-frequency correlation. Comput Electron Agr. 205, 107630 https://doi.org/10.1016/j.compag.2023.107630.

Weigand, M., Kemna, A., 2017. Multi-frequency electrical impedance tomography as a non-invasive tool to characterize and monitor crop root systems. Biogeosciences 14, 921–939. https://doi.org/10.5194/bg-14-921-2017.

Weigand, M., Kemna, A., 2019. Imaging and functional characterization of crop root systems using spectroscopic electrical impedance measurements. Plant and Soil 435, 201–224. https://doi.org/10.1007/s11104-018-3867-3.

Zajicova, K., Chuman, T., 2019. Application of ground penetrating radar methods in soil studies: A review. Geoderma 343, 116–129. https://doi.org/10.1016/j.geoderma.2019.02.024.

Zhao, K., 2008. Dielectric spectroscopy and its applications. Chemical Industry Press, Beijing China.